Supporting Information

High-throughput dielectrophoretic cell sorting assisted by cell sliding on scalable electrode tracks made of conducting-PDMS

Xiaofeng Nie[a], Yuan Luo[b,c], Penghui Shen[a], Chengwu Han[d], Duli Yu[a,e], Xiaoxing Xing[a,*]

[a] College of Information Science and Technology, Beijing University of Chemical Technology, No. 15 North 3rd Ring Rd., Beijing, 100029, China

[b] Department of Medical Engineering, California Institute of Technology, Pasadena, CA 91125, USA

[c] Department of Biomedical Engineering, School of Engineering, Southern University of Science and Technology, 1088 Xueyuan Avenue, Nanshan District, Shenzhen, 518055, China

[d] Department of Clinical Laboratory, China-Japan Friendship Hospital, No. 2 Yinghuayuan East Street, Chaoyang District, Beijing, 100029, China

[e] Beijing Advanced Innovation Center for Soft Matter Science and Engineering, No. 15 North 3rd Ring Rd., Beijing, 100029, China

[*]Correspondence: Xiaoxing Xing

College of Information Science and Technology

Beijing University of Chemical Technology

No. 15 North 3rd Ring Rd., Beijing, 100029, China

EMAIL: xxing@mail.buct.edu.cn

TEL: (+86) 15831675576

FAX: (+86) 6443 6719

Contents:

Supporting simulation results

Electric field distribution in the vertical direction

Specifically, the unique design of two-layer digit in our device, with posts undercutting the upper track layer, results in varied sidewall profile of the electrode, and thus it gives rise to an electric field non-uniform along the channel depth other than across the horizontal planes. In this way, our device generates spatially effective DEP force field in both the lateral and vertical directions. Such electric field non-uniformity in the vertical direction is critical for driving cells under pDEP to move upward from the lower layer to the upper track where the electric field peaks. The two-layer electrode digit with varied sidewall profile differentiates our device from the typical 3D volumetric electrodes composed of extrusion blocks featuring uniform sidewall profiles [22-24], which fail to induce electric field non-uniformity and thus DEP force along the channel depth. As shown in Fig. S2, we further compare the distributions of the electric field intensity and the $\nabla|E|^2$ magnitudes across a vertical plane cut tangentially along the electrode edge respectively for the 2D device, our device as well as a special case of our device with the track layer going through the entire chamber height without supporting posts. Compared to its 2D version (Fig. S2a), our device (Fig. S2b) offers more extended region under strong electric field and $\nabla|E|^2$ in this cutting plane, leading to DEP force influential in a greater range along the channel depth. The electrode design in Fig. S2c is analogous to the typical 3D volumetric electrodes with uniform sidewall profile, which projects uniform electric field and thus negligible DEP force field in the vertical plane. Notably, the posts in our device not only enable cell transition along the vertical direction by the DEP force, but also create flow paths penetrating the digit under the track.

Flow field simulation and the coupling of the electric field with the flow field

Fig. S3a and c respectively depict the flow velocity magnitudes overlapped with normalized velocity vectors in the horizontal cross-sectional plane-S and the vertical cross-sectional plane cut along C-C' (labeled in Fig. S3a). The fluid flow upon attacking the track, as indicated in Fig. S3a by the arrows in the horizontal plane-S, would be turned to a direction more tangential to the track, which gives rise to considerable drag force decomposed along the track and thus this drag force effectively drives the cells to slide. On the other hand, fluid passing a track will squeeze through the gaps between adjacent posts under the track. The flow consequently gains downward and upward velocities when respectively

approaching and leaving the gap, as further elucidated by the decomposed velocity vectors along z-axis in the lower panel of Fig. S3c. Such down/upward velocities lead to vertical drag forces that affect the vertical position of a sliding cell along the track.

The unique two-layer track electrode design of our device also facilitates the coupling of the electric field and the hydrodynamic flow field, which benefits more rapid lateral cell migration via sliding than the 2D device. In our device, as indicated by the arrows designating vertical DEP force in Fig. S2b, cells under pDEP that appear either higher near the ceiling or lower than the track would all be moved to the lower edge of the track, corresponding to a vertical position ~20 μm away from the chamber ceiling. Fig. S3a depicts the flow velocity profile with velocity vector arrows. The parallel facing sidewalls of adjacent tracks, serving also as fluid boundaries, twist the flow in the upper track layer to a beneficial direction nearly tangential to the track (arrows). Meanwhile, the track plates also slightly squeeze the fluid, which lead to moderate velocity magnitude. Therefore, cells loaded onto the track by pDEP experience effective fluid drag along the digit that drive them to slide. In contrast, the planar electrodes in the 2D device attract cells under pDEP toward the electrode edge on the chamber floor, where the flow becomes stagnant. Fig. S3b depicts the flow velocity profile at the horizontal plane 7.5 μm above the plane-S (i.e., the chamber floor). The height of this plane equals the vertical position of the spherical center for a cell with 7.5 μm radius, which is trapped on the electrode edge. The fluid proceeds downstream (arrows) straightly and the velocity magnitudes emerge to be much lower than that in our device (Fig. S3a). Such low velocity could lead to weak drag force decomposed to the direction along the digit, which drives the cells to move along the digits much slower than those sliding on the 3D track electrode in our device. It may even lead to cell stuck on the electrode edge as reported by the prior work in reference [8] that also separates cells in pDEP regime.

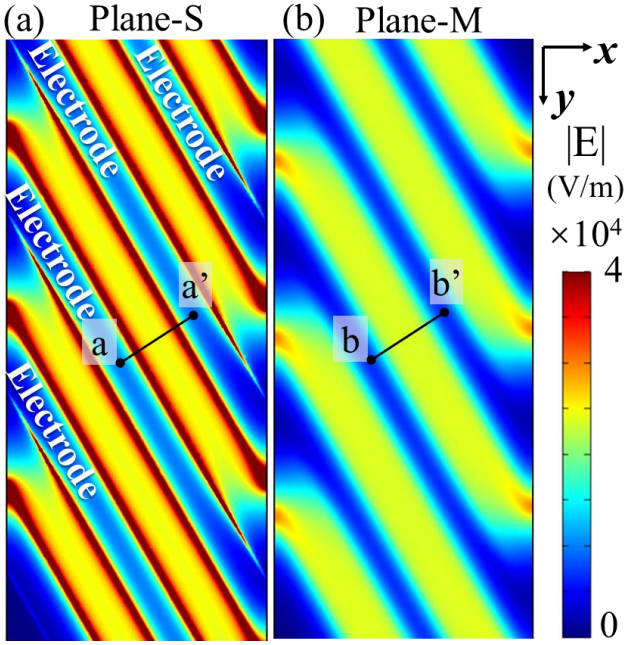

Fig. S1. Electric field distributions across the horizontal (a) plane-S and (b) plane-M for the 2D device.

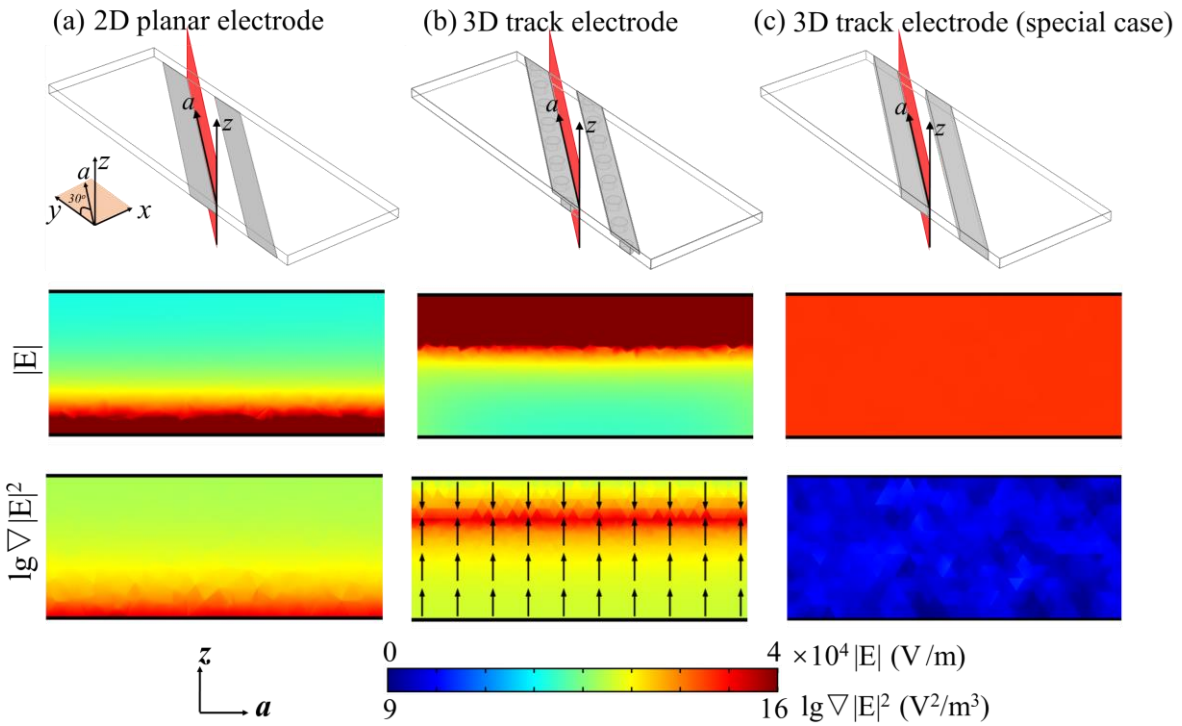

Fig. S2. Distributions of the electric field intensity and the $\nabla|E|^2$ magnitude in logarithmic scale across the vertical planes cut tangentially along the electrode edges of (a) the planar electrodes in the 2D device, (b) the 3D track electrodes in our device, and (c) the a special case of the 3D track electrodes with the track layer going through the entire channel depth without posts. Upper panels: schematic illustration for cutting the cross-sectional planes. Mid panels: color maps of electric field intensity. Lower panels: color maps of $\nabla|E|^2$ magnitude in logarithmic scale. Normalized arrows overlapped the color map of $\nabla|E|^2$ in (b) indicate the direction of the pDEP force along the z axis.

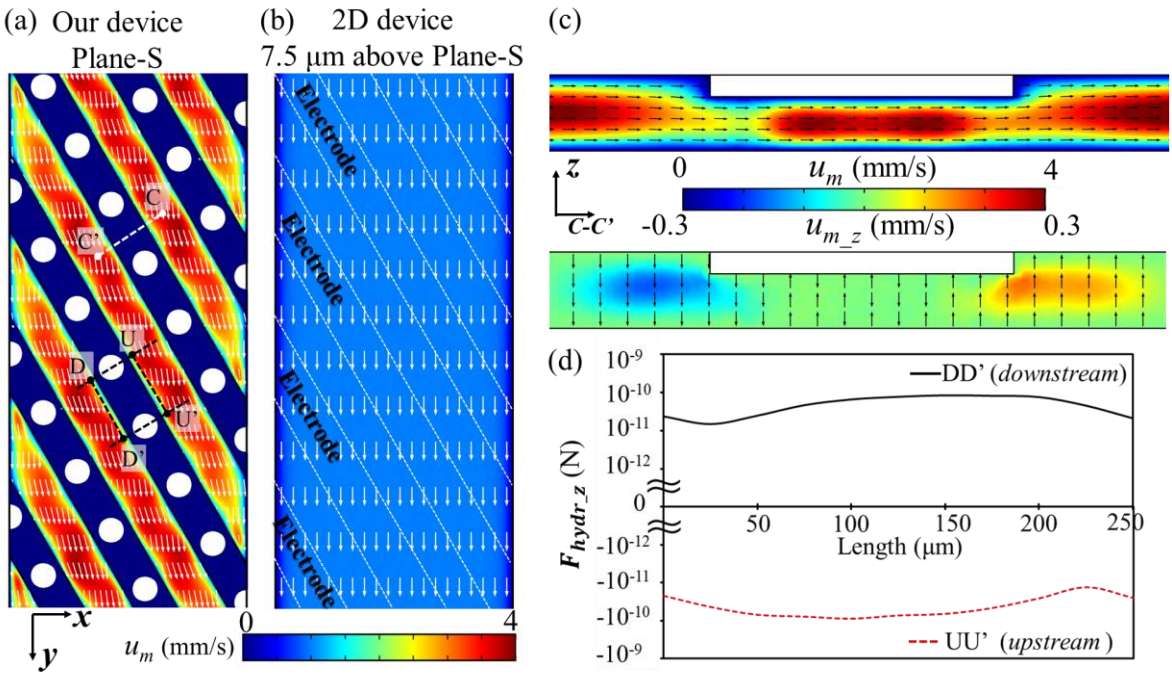

Fig. S3. (a-b) Flow velocity magnitudes (color map) and directions (uniform arrows) in horizontal planes of (a) the plane-S of our device and (b) the plane located 7.5 μm higher than the plane-S of the 2D device. (c) Flow velocity magnitudes and directions (upper panel) as well as the decomposed velocity in the vertical direction (lower panel) in the vertical plane cut along C-C' line in (a). (d) The vertical hydrodynamic force acting on a cell with respect to its spherical center shifting respectively along U-U' and D-D' in (a). The cell center is in plane-S of our device, and is separated with 7.5 μm distance from the track sidewalls facing up- or down-stream.

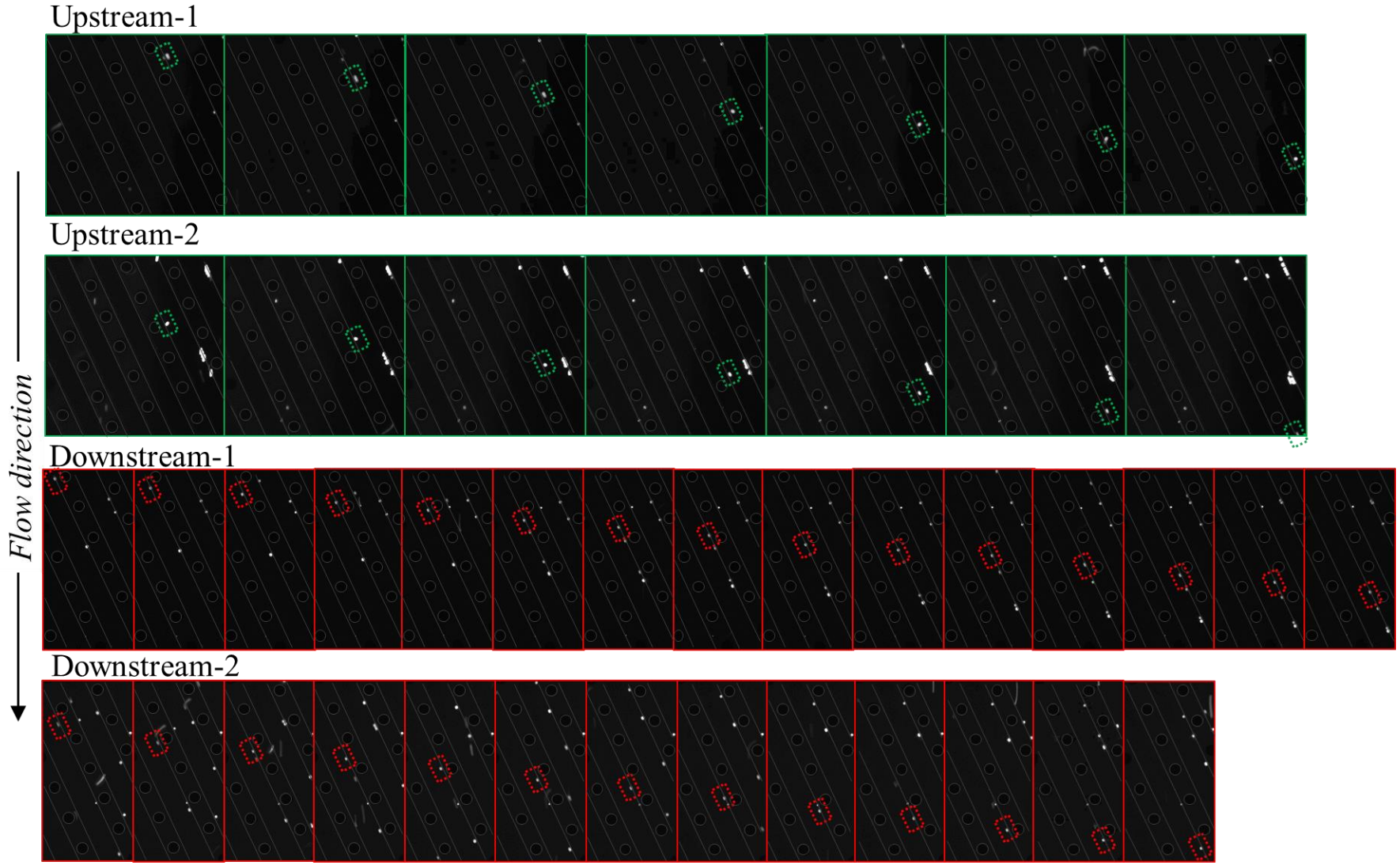

Fig. S4. Sequential micrographs illustrating four trajectories of sliding cells along upstream (green dashed box) and downstream (red dashed box) sides of electrode digits. Sample flow: 0.5 ml/h. Sheath flows: 0.5 ml/h. Activation signal: 15 V_p and 400 kHz. DEP buffer: 100 µS/cm.

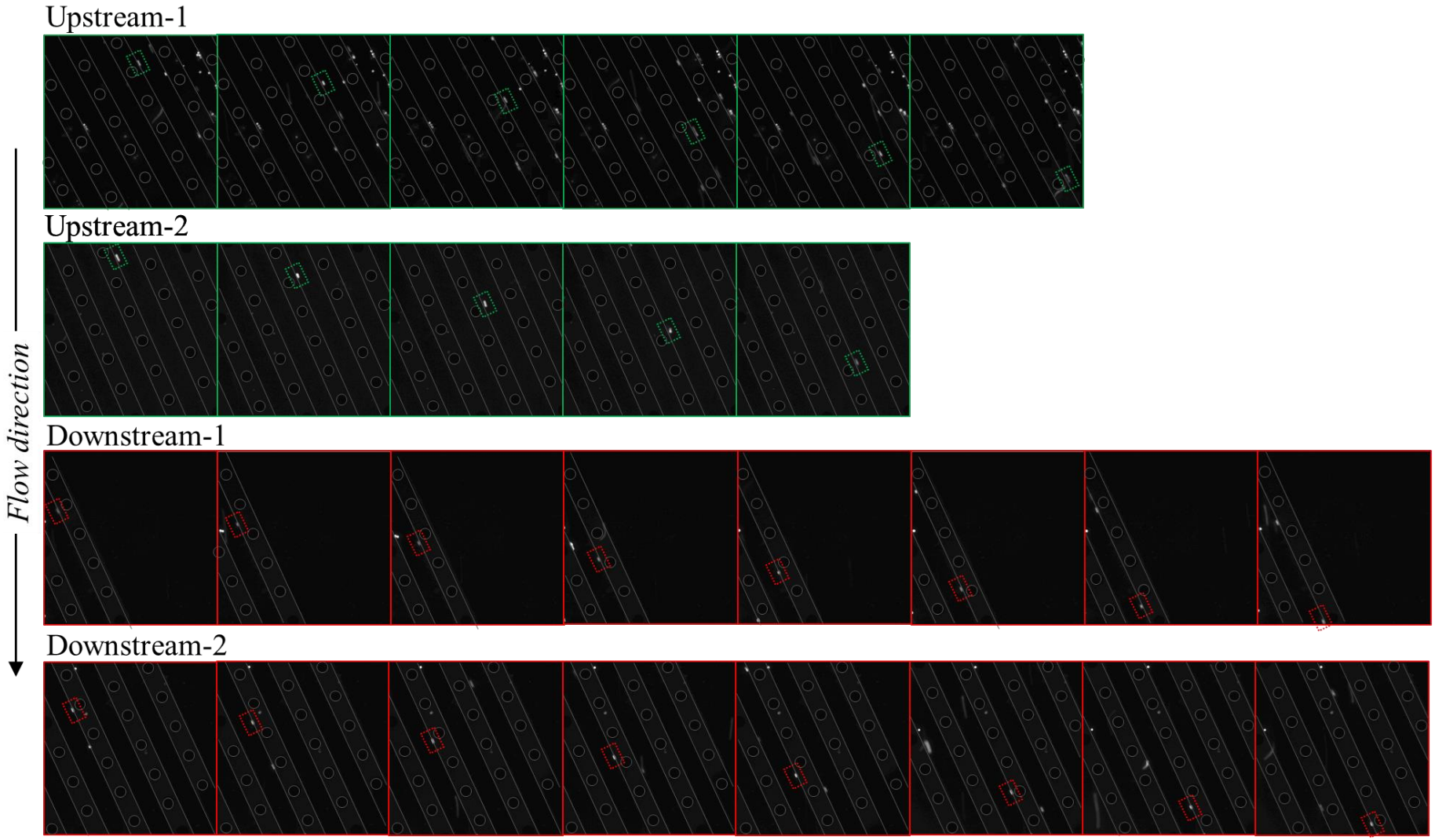

Fig. S5. Sequential micrographs illustrating four trajectories of sliding cells along upstream (green dashed box) and downstream (red dashed box) sides of electrode digits. Sample flow: 1 ml/h. Sheath flows: 0.5 ml/h. Activation signal: 15 V_p and 400 kHz. DEP buffer: 100 µS/cm.

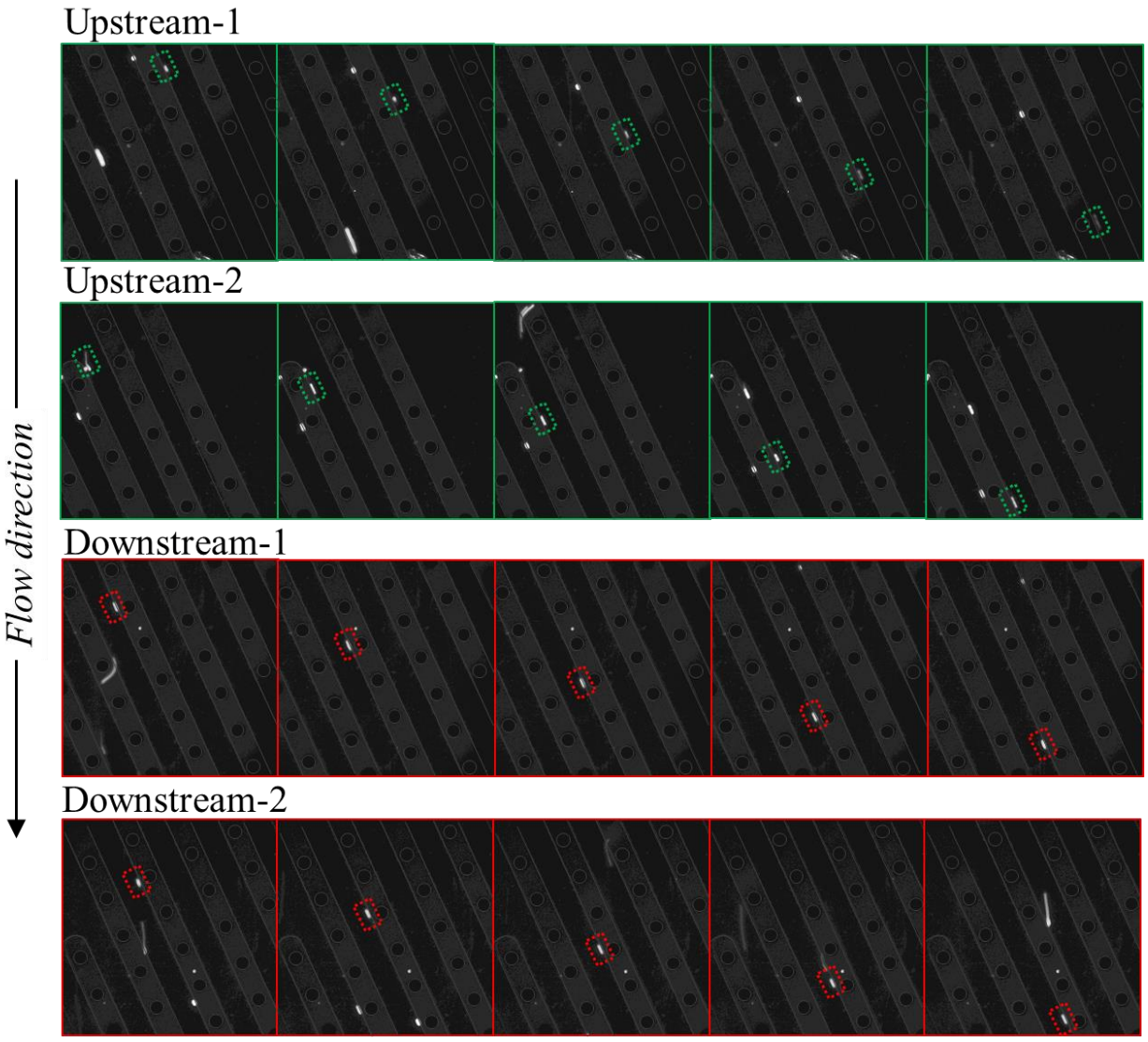

Fig. S6. Sequential micrographs illustrating four trajectories of sliding cells along upstream (green dashed box) and downstream (red dashed box) sides of electrode digits. Sample flow: 1.2 ml/h. Sheath flows: 0.5 ml/h. Activation signal: 15 V_p and 400 kHz. DEP buffer: 100 µS/cm.

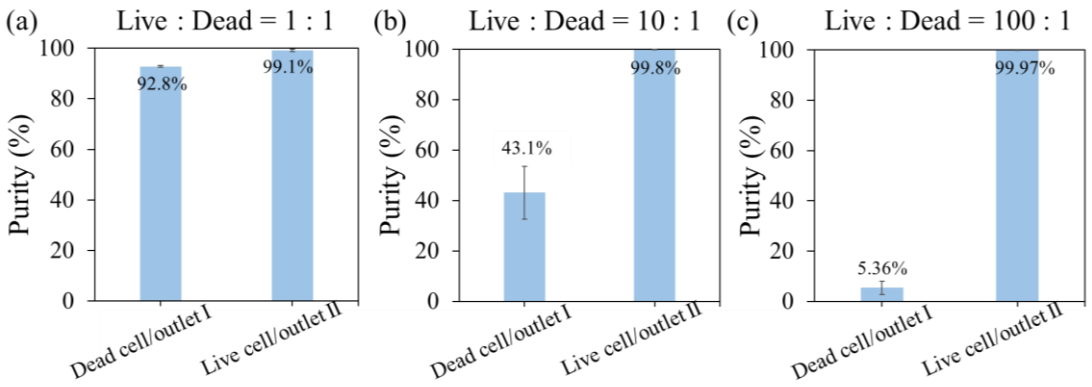

Fig. S7. The purities of live cells in outlet II and dead cell in outlet I in the unidirectional device with the concentration ratios (live cells: dead cells) in sample mixture at (a) 1:1 (b) 10:1 and (c) 100:1. The dead cell concentration was fixed at 1×10^5 cells/ml. Data symbols and error bars denote mean ± s.d. (n = 3). Sample flow rate: 1 ml/h. Sheath flow rate: 0.5 ml/h. Activation: 15 V_p and 400 kHz. DEP buffer: 100 μS/cm.

Movie

Video for continuous-flow separation of live (red) and dead (green) Hela cells using a unidirectional device. The live and dead cells, respectively with 1×10^6 and 1×10^5 cells/ml concentrations, were mixed in DEP buffer of 100 μS/cm. The sample and sheath flows were continuously infused into the device at 1 ml/h and 0.5 ml/h, respectively. The DEP activation was applied at 15 V_p and 400kHz. The video comprises superimposed image sequences separately taken from the midstream and outlet regions of the device before and after DEP onset. When DEP was off, both the live and dead cells in the sample flow were focused by the sheath to the left side of the chamber, penetrating the electrode digits under the track at midstream, and were subsequently delivered into the outlet I. With DEP onset, the live cells under strong pDEP got loaded onto both the up- and down-stream sides of the track and slid toward the right side of the chamber, where they were periodically released during the off-cycle of the activation voltage and finally exited the device via outlet II within an enriched stream. In comparison, the dead cells under weak DEP exhibited similar trajectories as when DEP was off and proceeded to the outlet I.